İSTANBUL UNIVERSITY CERRAHPAŞA

ORIGINAL ARTICLE
Electrica 2023; 23(2): 270-280

Robust-Proportional-Integral-Derivative Controller Design for Magnetic Levitation System Using Big Bang–Big Crunch Algorithm

Moayed Almobaied, Hassan S. Al-Nahhal, Khaled B.A. Issa

Department of Electrical Engineering, Islamic University of Gaza, Gaza, Palestine

Cite this article as: M. Almobaied, H. S. Al-Nahhal and K. B. Issa, "Robust-proportional-integral-derivative controller design for magnetic levitation system using big bang–big crunch algorithm," *Electrica*, 23(2), 270-280, 2023.

ABSTRACT

The proportional-integral-derivative (PID) controller is the most extensively used methodology in industrial control systems among control loop feedback mechanisms. The calculation of PID controller gains (K_P,K_D,K_I) is the traditional PID controller synthesis. In order to construct a robust stability system, the parameter space technique is elected to determine all of the PID's parameters. In fact, the results of the parameter space approach are ranges of PID gains (K_P,K_D,K_I). The Big Bang–Big Crunch optimization algorithm is proposed here to optimize a time domain fitness function in the design of the PID control, ultimately avoiding PID parameters that do not fulfill the performance index function. The optimization approach is presented in this work via a specific performance index function that is inversely proportional to a dynamical system's time-domain step response criteria. The feasibility of the proposed graphic method for achieving robust stability for magnetic levitation systems has been illustrated using MATLAB simulations.

Index Terms—Affine polynomial, Big Bang–Big Crunch, Maglev, proportion al-integral-derivative, robust, uncertain parameters

I. INTRODUCTION

Many researchers in the control engineering field consider the stabilization of nonlinear systems as a challenging problem. One of the most popular benchmarks that have a high nonlinearity is magnetic levitation (Maglev) [1]. Magnetic levitation is a mechanism for suspending a target in space by manipulating magnetic force, which is used to counteract the target's gravitational force [2]. With high nonlinearity, the mathematical model of Maglev systems is unstable. As a result, there is significant competition for research in research centers and universities on modeling and control. The linearized model and the nonlinear model are two well-known modeling methodologies that can be found in the literature. For the linearized model, Proportional-Integral (PI), proportional-integral-derivative (PID), fuzzy, and Linear–Quadratic-Regulator (LQR) approaches are commonly utilized [3–5]. Proportional-integral-derivative is the simplest and most straightforward of these strategies to create and execute. The biggest disadvantage of the PID controller is the tuning technique for the values of PID parameters. On the other hand, sliding mode control with output feedback is a powerful method for nonlinear perspectives [6–8]. Actually, neither of the aforementioned conventional methodologies considers the proposed controller's robustness in the presence of parametric uncertainty in the system. One of the most important branches of the robust control discipline is the study of complicated systems with parametric uncertainty. Any linear uncertain system's characteristic polynomials contain one or more uncertain parameters that appear at the polynomial coefficients of the characteristic equation in the model's transfer function. The polynomial family is categorized into interval coefficients, affine linear coefficients, multilinear coefficients, and polynomial coefficients, with the classification based on how uncertain factors are included into the polynomial coefficients [9]. In [1], the authors show how to use the parameter space approach to determine all stabilizing PID parameters (K_P,K_I,K_D) for the Maglev ED-4810 system with parametric uncertainties which its characteristic polynomial is of the affine type, meaning that the uncertain parameters enter the coefficients of the characteristic polynomial linearly. In [10], a genetic optimization algorithm (GA) was utilized to tune the optimal PID parameters that result in the optimal performance indices for a Maglev system. A new low computational burden design is proposed to adjust the gains of the hybrid discrete-time Laguerre function and the model predictive control based on the social

The content of the manuscript has been presented before in the paper "Computation of Stabilizing PID Controllers for Magnetic Levitation System with Parametric Uncertainties," which illustrates the calculation of all stabilizing PID controller gains for ED-4810 magnetic levitation system benchmark (Maglev) in the presence of uncertain parameters, at the 2021 International Conference on Electric Power Engineering (ICEPE-P), Gaza, Palestine on March 23–24, 2021.

Corresponding author:
Moayed Almobaied

E-mail:
malmobaied@iugaza.edu.ps

Received: June 22, 2022

Revised: October 1, 2022

Accepted: October 19, 2022

Publication Date: December 10, 2022

DOI: 10.5152/electrica.2022.22070

ski driver algorithm, which is devoted to delivering effective steering control for autonomous vehicles [11]. The model predictive controller variables are tuned using the arithmetic optimization approach to regulate an automatic voltage regulator [12]. For a nuclear reactor power system, the lightning search algorithm-based variable structure controller architecture is recommended [13]. For a nonlinear load frequency controller of a power system, the artificial bee colony (ABC) is implemented to optimize the variables of the PID [14]. The modified multitracker optimization algorithm is presented for the robotic manipulator to adjust the nonlinear model predictive control parameters [15]. Traditional optimization techniques are founded on presumptions such as differentiability, the cost function's convexity, and the requirements that have to be fulfilled. As these presumptions are difficult to satisfy through restricted optimization and to simplify the process of tuning control factors, several innovative heuristic algorithms, including Big Bang–Big Crunch (BB–BC) algorithm [16], ABC algorithm [17, 18], and teaching-learning-based optimization (TLBO) algorithm [17], have been established. Due to its high capability for optimization techniques, BB–BC algorithm has attracted a significant amount of attention from control systems experts in order to get the optimum parameters for several control schemes. It is derived from one of the physics and astronomy concepts about the evolution of the universe [16]. The BB–BC has been used in this study to adjust the PID parameters (K_P,K_I,K_D) for the Maglev system. The maximum and minimum values of PID gains (K_P,K_I,K_D) are determined by a parameter space technique. By contrasting the results with the ABC and TLBO algorithms, the results for settling time, overshoot, and steady-state error are verified.

The following is how the remainder of this paper is structured. Section II introduces ED-4810 Maglev mathematical modeling and problem formulation. In section III, the suggested robust PID controller is designed, and the set of all PID stabilizing domains is demonstrated. In section IV, the BB–BC optimization algorithm is described. The hypothesized BB–BC optimization approach for PID controller is presented in Section V. In section VI, the simulation results are discussed to demonstrate the validity of the proposed graphical methodology. Finally, in section VII, concluding remarks are expressed.

II. MAGNETIC LEVITATION MODELING

Fig. 1 shows the model of the ED-4810 Maglev, which allows theoretical confirmation of the principle of Maglev by suspending a steel ball in the air using a magnetic force. Due to the obvious significant nonlinearity in its model, this system is safe for university laboratories and may be used to examine the effectiveness of various types of controllers [19].

Equation (1) presents the relationship between the coil's voltage and current mathematically.

$$e(t) = Ri(t) + L\frac{di(t)}{dt} \tag{1}$$

where

m: weight of steel ball

$y(t)$: center position of the ball

$i(t)$: electric current flowing on an electromagnetic coil

c: magnetic force constant

L: inductance of wire

R: resistance of wire

$e(t)$: input voltage.

The total sum of the forces acting on the vertical depicted in Fig. 1 is:

$$f_{total} = f_{gravity} + f_{em} \tag{2}$$

where $f_{gravity}$ is the force of gravity and the upper coil's electromagnetic force is represented by this symbol f_{em}.

The mathematical model of the physical system shown in Fig. 1 is represented by the first-order differential equations as follows:

$$m\ddot{Y} = mg - c\frac{i^2}{y} \tag{3}$$

$$\dot{x}_a = x_b \tag{4}$$

$$\dot{x}_b = g - \frac{cx_c^2(t)}{mx_a} \tag{5}$$

$$\dot{x}_c = \frac{-R}{L}x_c(t) + \frac{1}{L}u(t) \tag{6}$$

where $x_a = y(t)$ is the distance of the ball, $x_b = \dot{y}$ is defined as the velocity of the ball, $x_c = i(t)$ is defined as the coil's current, and $u(t) = e(t)$ is the input voltage.

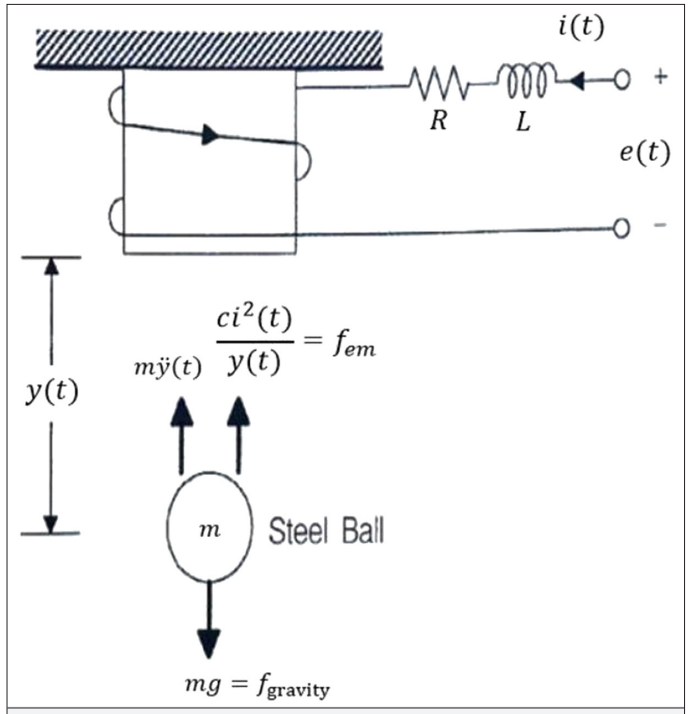

Fig. 1. Magnetic levitation system model.

The previously stated equations can be arranged in state space format for flexibility of use, as demonstrated in (7) [19].

$$\begin{bmatrix}\dot{x}_a\\ \dot{x}_b\\ \dot{x}_c\end{bmatrix}=\begin{bmatrix}0 & 1 & 0\\ \frac{g}{x_a} & 0 & \frac{-cx_c}{mx_a}\\ 0 & 0 & -\frac{R}{L}\end{bmatrix}\begin{bmatrix}x_a\\ x_b\\ x_c\end{bmatrix}+\begin{bmatrix}0\\ 0\\ \frac{1}{L}\end{bmatrix}u(t) \tag{7}$$

The resulting state space model is obviously nonlinear. As a result, in order to use the proposed method, these equations must be linearized. The following assumptions are taken into account throughout the linearization process:

- $x_a = x_1 = y^*$, where x_1 is the distance of the ball and y^* is defined as its center equilibrium point.
- $x_b = x_2 = 0$ is defined as the velocity of the ball.
- $\dot{x}_b = 0$ is defined as the acceleration of the ball.
- $x_c = x_3$ is defined as the current $i(t)$ and $\dot{x}_c = 0$.

Hence, the value of x_c can be calculated from (3) as:

$$x_c = x_3 = i^* = \sqrt{\frac{mgy^*}{c}} \tag{8}$$

According to the standard methods for linearization, which are detailed in [19], the resultant linearized state space model will be as follows:

$$\begin{bmatrix}\dot{x}_a\\ \dot{x}_b\\ \dot{x}_c\end{bmatrix}=\begin{bmatrix}0 & 1 & 0\\ \frac{g}{y^*} & 0 & \frac{-2}{y^*}\sqrt{cg/m}\\ 0 & 0 & -\frac{R}{L}\end{bmatrix}\begin{bmatrix}x_a\\ x_b\\ x_c\end{bmatrix}+\begin{bmatrix}0\\ 0\\ \frac{1}{L}\end{bmatrix}u(t) \tag{9}$$

$$y(t)=\begin{bmatrix}1 & 0 & 0\end{bmatrix}\begin{bmatrix}x_a\\ x_b\\ x_c\end{bmatrix} \tag{10}$$

The linearized state space model's resultant transfer function is:

$$G(S)=\frac{\sqrt{\frac{4ycg}{m}}}{-LyS^3-RyS^2+LgS+gR} \tag{11}$$

Both R and L were chosen as the uncertain parameters in this research, and the values of the other parameters are listed in Table I.

Therefore, by substituting the values of Table I in (11), the transfer function will be:

$$G(s)=\frac{42}{-3LS^3-3RS^2+980LS+980R} \tag{12}$$

The characteristic polynomial of the transfer function in (12) is:

$$P(S,R,L)=-3LS^3-3RS^2+980LS+980R \tag{13}$$

TABLE I. THE CERTAIN PARAMETERS VALUES OF ED-4810 MAGNETIC LEVITATION SYSTEM [19]

Parameters	Values	Units
M	2	kg
G	9.8	m/s^2
C	0.3	-
$y*$	0.03	M
$i*$	1.44	A

The aforementioned polynomial family belongs to the affine polynomial class, in which the uncertain parameters R and L linearly enter the polynomial coefficients that have the following ranges:

$R \in [45,55], L \in [0.15,0.25]$The uncertain parameters in robust control theory are symbolized by the letters q, i.e., $q_1 \triangleq R$, $q_2 \triangleq L$.

Therefore, the characteristic equation can be expressed as:

$$P(S,q_1,q_2)=-3q_2S^3-3q_1S^2+980q_2S+980q_1 \tag{14}$$

III. ROBUST PROPORTIONAL-INTEGRAL-DERIVATIVE CONTROLLER DESIGN

Many methods, such as Ziegler Nichols and Nyquist procedures, have been utilized in the literature to tune PID controllers. The designers will only have one set of values for the PID parameters (K_P, K_I, and K_D) using these traditional procedures. A parameter space approach, on the other hand, is a graphical strategy for identifying all PID parameter stability regions and is considered an excellent tool for robust stabilization problems.

Equation (15) demonstrates the open loop uncertain transfer function found in (12) where the resistance R and the inductance L were replaced by q_1 and q_2, respectively.

$$G(s)=\frac{42}{-3q_2s^3-3q_1s^2+980q_2s+980q_1} \tag{15}$$

where $q_1 \in [45,55]$, $q_2 \in [0.15,0.25]$. Equation (16) represents the traditional PID controller's transfer function.

$$G(s)=\frac{K_DS^2+K_PS+K_I}{S} \tag{16}$$

A. Hurwitz Stabilizing Proportional-Integral-Derivative Controller

Fig. 2 demonstrates the closed-loop PID controller for the Maglev system, where R and L are selected as 50 Ω and 0.2 H, respectively.

Hence, the closed-loop characteristic polynomial is as follows:

$$P(S,K_D,K_P,K_I)=-3S^4-750S^3+(210K_D+4980)S^2+(210K_P+245000)S+210K_I \tag{17}$$

The parameter space technique is one method for locating stability regions in the parameter space when mapping the stability

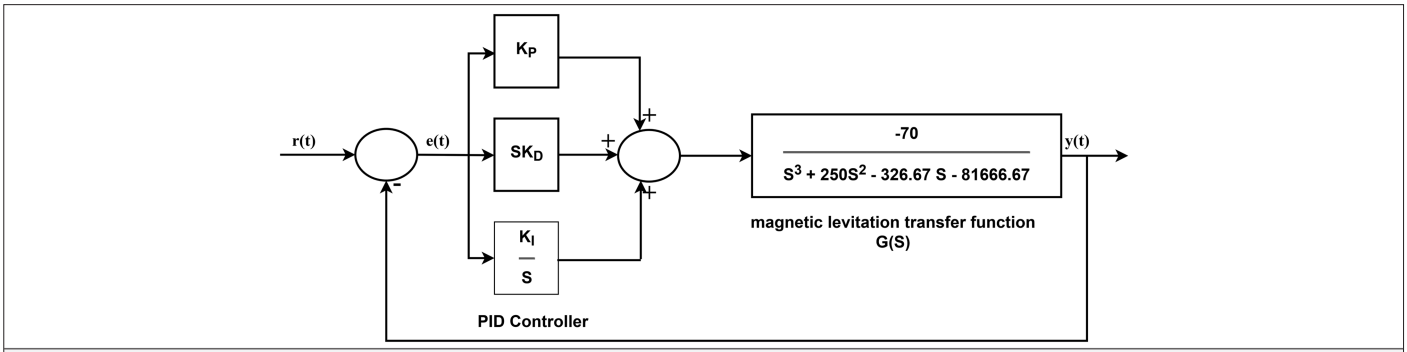

Fig. 2. The magnetic levitation system's closed-loop proportional-integral-derivative controller.

border to the parameter space [20]. For $P(S,K_D,K_P,K_I)$, the Real and Imaginary parts are:

$$Real = 210K_I - 210\omega^2 K_D - 3\omega^4 - 980\omega^2 \tag{18}$$

$$Img = 750\omega^3 + 245000\omega + 210K_P)\omega \tag{19}$$

The two equations earlier are arranged in the matrix form as follows:

$$\begin{bmatrix} 210 & -210\omega^2 \\ 0 & 0 \end{bmatrix}\begin{bmatrix} K_I \\ K_D \end{bmatrix} + \begin{bmatrix} -3\omega^4 - 980\omega^2 \\ 750\omega^3 + (245000 + 210K_p)\omega \end{bmatrix} = 0 \tag{20}$$

When there are only two variables to examine, the parameter space approach is truly a decent option. If the parameter space includes more than two parameters, one methodology to visualize stability areas is to fix all except two among parameters. In the case of PID controllers, there is indeed a special scenario where it is possible to demonstrate that the stabilizing zones for a fixed K_P value are polygonal in shape [9]. Equation (20) is manifestly of the form $Ax+b=0$, and the determinant of matrix A should not equal zero in order to find a solution. The determinant of the matrix A in (20) will be as follows:

$$Det(A) = \begin{vmatrix} 210 & -210\omega^2 \\ 0 & 0 \end{vmatrix} \tag{21}$$

For whichever ω, the above determinant vanishes. As a result, instead of a point, the graphical solution for K_I and K_D in (18) and (19) seems to be either parallel lines or identical in the parameter plane. To ensure that the two lines are identical, the value of the parameter K_P must be specified within a range as follows.

$$\frac{0}{210} = \frac{0}{210\omega^2} = \frac{750\omega^3 + (245000 + 210K_P)\omega}{-3\omega^4 - 980\omega^2} \tag{22}$$

Then,

$$\omega^2 = -\frac{245000 + 210K_P}{750} \tag{23}$$

Since the frequency should be positive, the value of K_P is obtained so that $(245000 + 210KP) \le 0$. As a result, $K_P < -1166.7$ is the condition to ensure that the lines in (18) and (19) are identical. The value of ω is equal to $\sqrt{2}$ when $K_P = -1173.8$ is utilized, as shown in (22) or Fig. 3, which visually depicts the relationship between K_P and ω.

By substituting the value of K_P in (18) and (19), we get:

$$Real = 210K_I - 210\omega^2 K_D - 3\omega^4 - 980\omega^2 \tag{24}$$

$$Img = 750\omega^3 - 1500\omega \tag{25}$$

The stability areas of both K_I and K_D for $P(s)$ are demonstrated in Fig. 4 where:

1. Real root boundary (RRB) at $\omega = 0$ is $K_I = 0$.
2. Infinity root boundary (IRB) at $\omega = \infty$ does not exist.
3. Complex root boundary (CRB) at $\omega = \sqrt{2}$:

$$210K_I - 420K_D = 1972 \tag{26}$$

The curves of Fig. 4 separate the plot into four distinct regions. According to the Boundary Crossing Theorem, if one of these regions has a stable polynomial, the rest of the region must also contain stable polynomials. If one of these regions contains an unstable

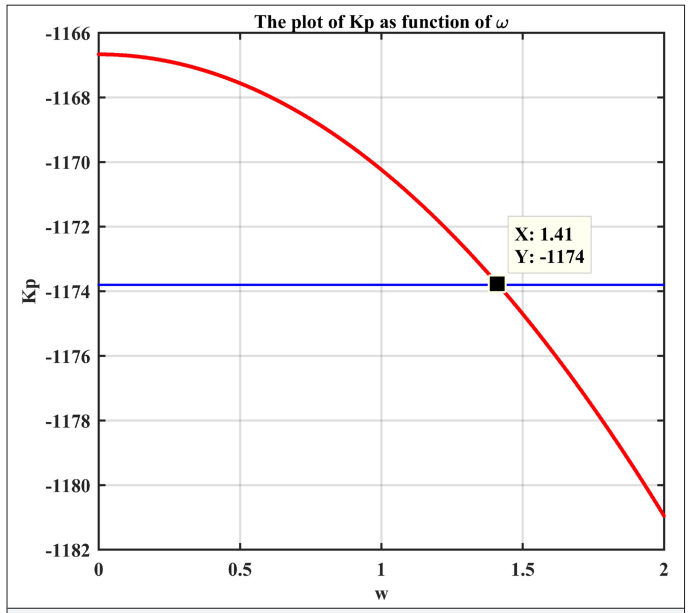

Fig. 3. K_P as function of ω for $P(s)$.

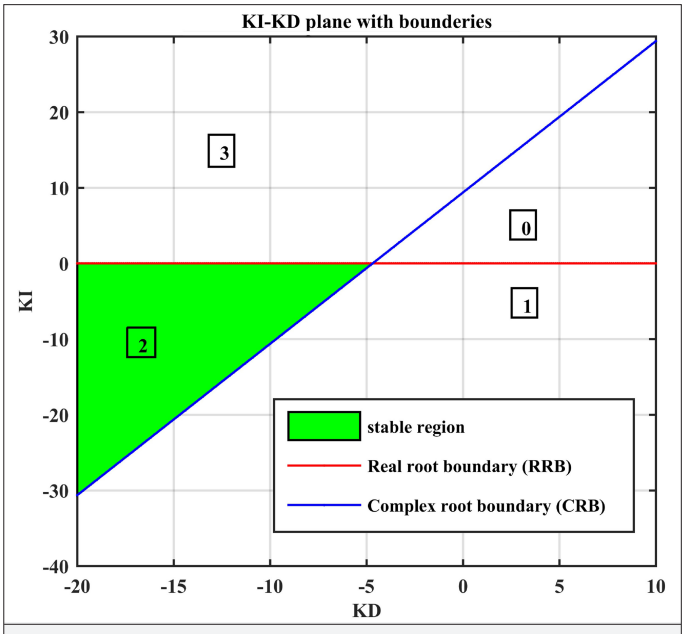

Fig. 4. K_I and K_D for $P(s)$.

polynomial, the rest of the region must be unstable polynomials. As a result, the set of stability zones may be thoroughly characterized by selecting one polynomial for each region and testing its stability [12]. When this procedure is applied to the graph in 8b, it is clear that there is only one stable zone.

B. Robust Stabilization Proportional-Integral-Derivative Controller

The closed loop PID controller for the uncertain Maglev system is illustrated in Fig. 5. If R and L are uncertain parameters, PID coefficients can be computed as follows:

As a consequence, the closed loop characteristic is:

$$P(S,q_1,q_2)=-3q_2S^4-3q_1S^3+(980q_2+42K_D)S^2+(980q_1+42K_P)S+42K_I) \quad (27)$$

In order to apply Khartinove's theorem for stability, the polynomial family should belong to the interval class [21]. In transforming the affine polynomial to interval one, the coefficients can be over-bounded. This can be accomplished by assuming that the affine polynomial coefficients are independent [9]. Although this strategy is conservative, it achieves a good result. Because the closed loop polynomial family in (27) is of order four, testing only two polynomials will be sufficient to ensure stability in the sense of Khartinove's theorem [9]:

$$P^{+-}(S,q)=a_0^+(q)+a_1^-(q)S+a_2^-(q)S^2+a_3^+(q)S^3+a_4^+(q)S^4 \quad (28)$$

$$P^{++}(S,q)=a_0^+(q)+a_1^+(q)S+a_2^-(q)S^2+a_3^-(q)S^3+a_4^+(q)S^4 \quad (29)$$

where $a_i^+(q)$ and $a_i^-(q)$ are the maximum and the minimum value of the coefficients, respectively, $q^-\le q\le q^+$ and $i=0,1,2,3,4$.

The requisite polynomials to test the stability can be found by substituting the specified parameters in (28) and (29):

$$P^{+-}=-0.45S^4-135S^3+(147+42K_D)S^2+(44100+42K_D)S+42K_I \quad (30)$$

$$P^{++}=-0.45S^4-165S^3+(147+42K_D)S^2+(43900+42K_P)S+42K_I \quad (31)$$

For both of the previous polynomials, the parameter space technique is utilized to locate the stability areas [9]. The Real and Imaginary components of P^{+-} when we replace S by $j\omega$ are as follows:

$$P_{Real}^{+-}=-0.45\omega^4-(147+42K_D)\omega^2+42K_I \quad (32)$$

$$P_{Img}^{+-}=135\omega^3+(44100+42K_P)\omega \quad (33)$$

The two equations earlier are organized in a matrix as follows:

$$\begin{bmatrix}42 & -42\omega^4\\ 0 & 0\end{bmatrix}\begin{bmatrix}K_I\\ K_D\end{bmatrix}+\begin{bmatrix}-0.45\omega^4-147\omega^2\\ 135\omega^3+(44100+42K_P)\omega\end{bmatrix}=0 \quad (34)$$

Similarly, in (32) and (33), the graphical solution for K_I and K_D is either parallel lines or identical in the parameter plane instead of a point. To ensure that the two lines are similar, the value of the parameter K_P must be specified within a range.

$$\frac{0}{42}=\frac{0}{42\omega^2}=\frac{135\omega^3+(44100+42K_P)\omega}{-0.45\omega^4-147\omega^2} \quad (35)$$

Then,

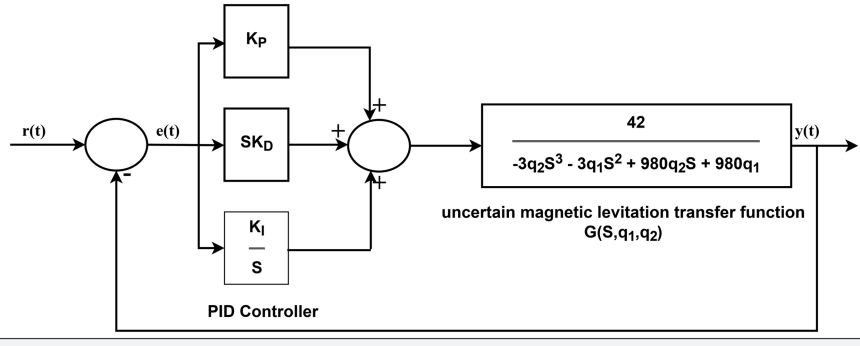

Fig. 5. The uncertain magnetic levitation system's closed loop proportional-integral-derivative controller.

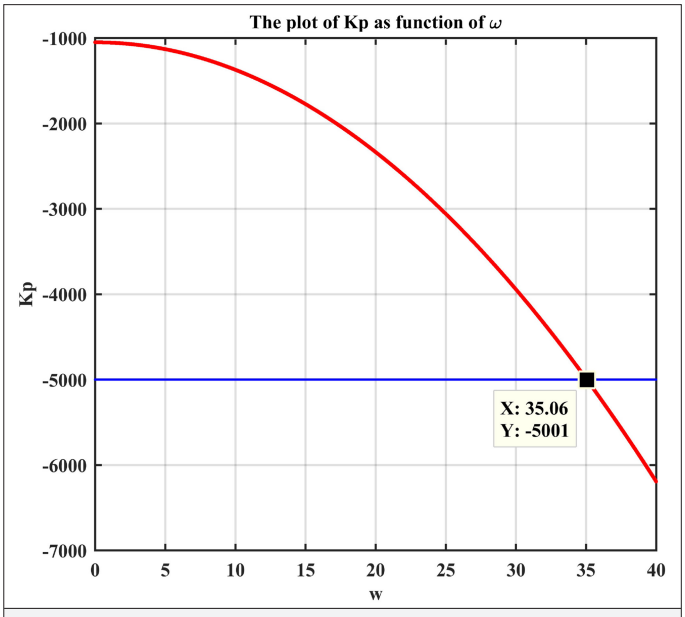

Fig. 6. K_p as function of ω for P^{+-}.

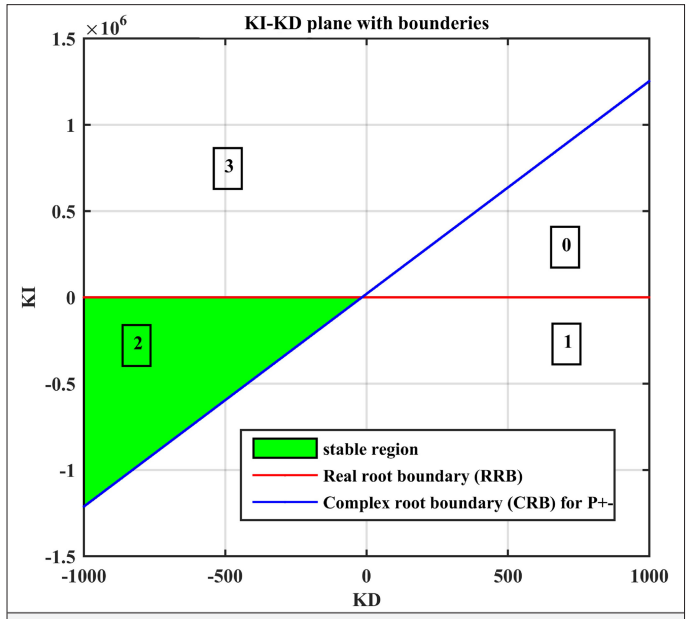

Fig. 7. K_I and K_D plane for P^{+-}.

$$\omega^2 = -\frac{44100 + 42K_P}{135} \tag{36}$$

$(44100 + 42KP) \le 0$ is the value of K_P that is picked. As a result, $K_P < -1050$ is the condition to ensure that the lines in (32) and (33) are identical. The value of ω is equivalent to 35.1 when $K_P = -5000$ is used, as seen in (36) or Fig. 6, which graphically depicts the relationship between K_P and ω.

By substituting the value of K_P in (32) and (33) we get:

$$P_{Real}^{+-} = -0.45\omega^4 - (147 + 42K_D)\omega^2 + 42K_I \tag{37}$$

$$P_{Img}^{+-} = 135\omega^3 - 2160\omega \tag{38}$$

The stability regions of both K_I and K_D for P^{+-} are shown in Fig. 7, where:

1. RRB at $\omega = 0$ is $K_I = 0$.
2. IRB at $\omega = \infty$ does not exist .
3. CRB at $\omega = 35.1$:

$$42K_I - 51744.4K_D = 688191.6 \tag{39}$$

There is just one stable region, as seen by the curves in Fig. 7.

The methodologies detailed earlier should be repeated for the P^{++} polynomial family, where:

$$P_{Real}^{++} = -0.45\omega^4 - (147 + 42K_D)\omega^2 + 42K_I \tag{40}$$

$$P_{Img}^{++} = 165\omega^3 + (43900 + 42K_P)\omega \tag{41}$$

These two equations have the following matrix form:

$$\begin{bmatrix} 42 & -42\omega^4 \\ 0 & 0 \end{bmatrix} \begin{bmatrix} K_I \\ K_D \end{bmatrix} + \begin{bmatrix} -0.45\omega^4 - 147\omega^2 \\ 165\omega^3 + (43900 + 42K_P)\omega \end{bmatrix} = 0 \tag{42}$$

For both P^{++} and P^{+-}, Fig. 8 illustrates the link between K_P and ω.

The value of K_P for P^{++} should be smaller than -1045. As a consequence, we chose $K_P = -5000$ as the value of K_P to meet both conditions in P^{++} and P^{+-}, with the consequent ω for P^{++} equal to 31.77. As a result, (40) and (41) can be reformed by adjusting the value of K_P as:

$$P_{Real}^{++} = -0.45\omega^4 - (147 + 42K_D)\omega^2 + 42K_I \tag{43}$$

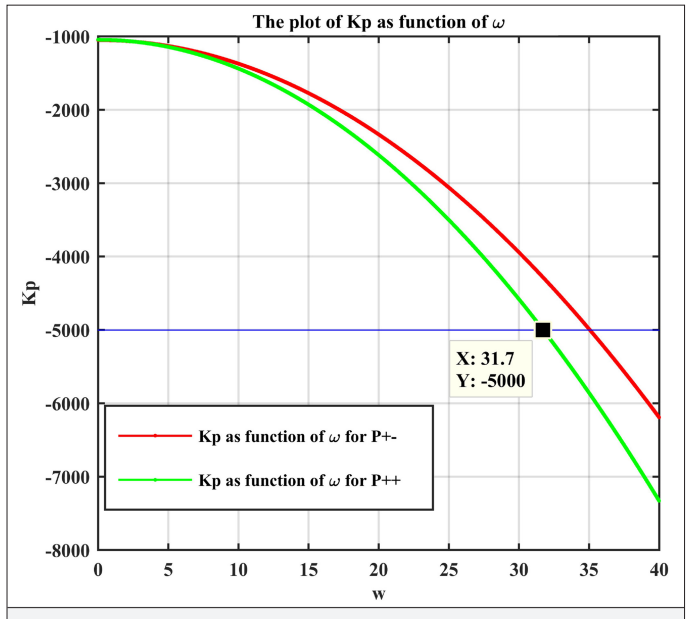

Fig. 8. K_P as function of ω for both P^{++} and P^{+-}.

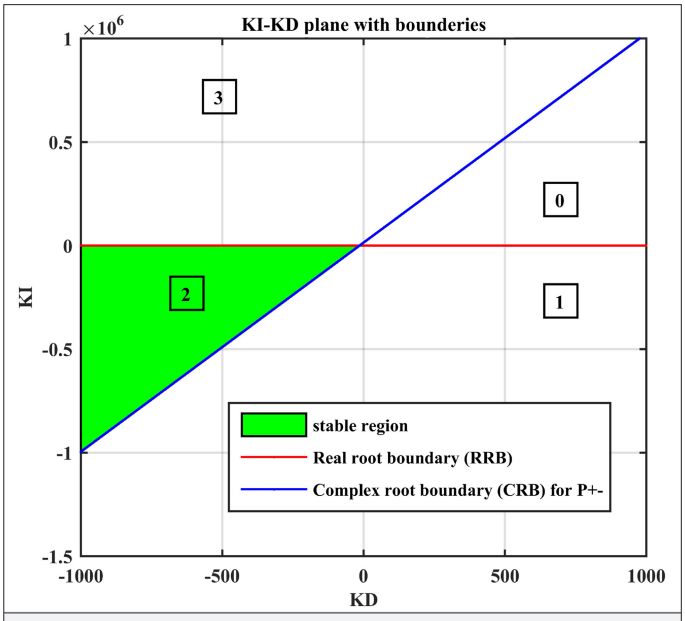

Fig. 9. K_I and K_D plane for P^{++}.

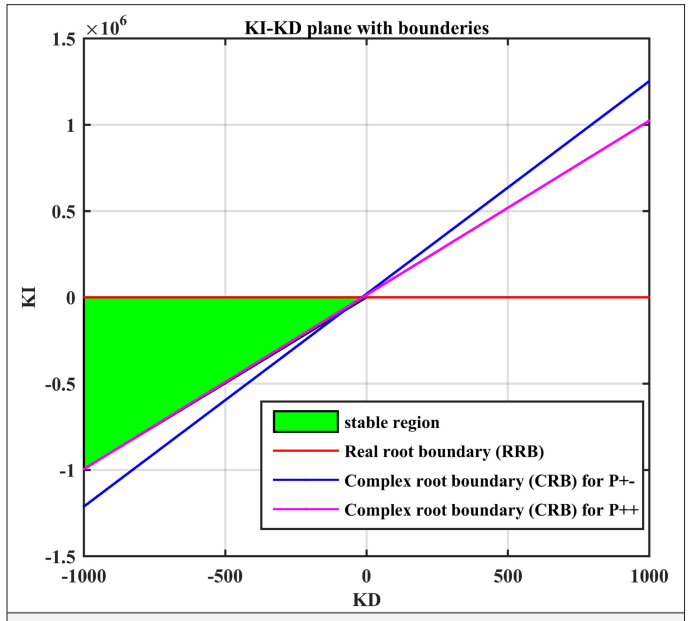

Fig. 10. K_I and K_D plane for P^{++} and P^{+-}.

$$P_{img}^{++} = 165\omega^3 - 2360\omega \tag{44}$$

The stability regions of K_I and K_D for P^{++} are shown in Fig. 9, where:

1. RRB at $\omega = 0$ is $K_I = 0$.
2. IRB at $\omega = \infty$ does not exist.
3. CRB at $\omega = 31.77$.

$$42K_I - 42258.65K_D = 603465 \tag{45}$$

The RRB and CRB lines for P^{++} also divide the "$K_I - K_D$" plane into new four separate areas, as seen in Fig. 9. As a result, the stable area of P^{++} may be identified in the same way as in the prior scenario.

We may establish that the stability region for P^{++} is a subset of the one for P^{+-} by comparing the stability regions for both P^{+-} and P^{++} in Fig. 10. As a result, the stability section for the original polynomial family is guaranteed by the stability region of P^{++} .

IV. BIG BANG–BIG CRUNCH OPTIMIZATION ALGORITHM

Erol and Eksin came up with the BB–BC algorithm [18]. The Big Bang hypothesis, an evolutionary theory that describes the origins of the cosmos, inspired the name of the algorithm. According to this concept, the algorithm has two phases: The Big Bang phase, in which candidate solutions are pulled toward irregularity across the search space, and the Big Crunch phase, in which candidate solutions are converged on a specific direction via a population center of mass. As the introductory Big Bang, the candidate solutions for the BB–BC algorithm are distributed randomly. In fact, only the first population is generated at random in the search space, but each Big Bang phase is preceded by a Big Crunch phase. All subsequent Big Bang phases are dispersed in an orderly manner around the center of mass. The outcomes of a Big Bang phase, on the other hand, will be inputs into a Big Crunch phase, which will only yield one output. The convergence operator of the candidate solution locations that it is the output of a Big Crunch phase can be defined as the center of mass. The center of mass is denoted by x^c, which can be expressed as follows:

$$\overleftarrow{x^c} = \frac{\sum_{i=1}^{N} \frac{1}{\overleftarrow{f^i}} \overleftarrow{x^i}}{\sum_{i=1}^{N} \frac{1}{\overleftarrow{f^i}}} \tag{46}$$

where x^i is a point in an n-dimensional search space produced, f^i is the value of this point's performance index function, and N is the population size in the Big Bang phase. The next step is to generate new points that will be employed in the Big Bang phase after the Big Crunch phase, which yields the center of mass x^c .The fresh production of these points will be redistributed in each direction around the center of mass x^c :

$$x^{new} = x^c + \frac{r\alpha\left(x_{max} - x_{min}\right)}{k} \tag{47}$$

where r is a random number, α is a parameter that limits the size of the search space, and k is the number of iterations. The center of mass is recalculated for the next step when new points are constrained to both up and down. The sequence of explosions and contractions is repeated until the halting requirement is fulfilled. The BB–BC optimization algorithm has the advantages of a short computation time and a fast convergence speed [16, 22–25].

V. BIG BANG–BIG CRUNCH OPTIMIZATION FOR PROPORTION AL-INTEGRAL-DERIVATIVE CONTROLLER

The BB–BC optimization algorithm is employed to optimize the (K_P, K_D, K_I) PID gains controller in this research. By using a parameter space method, the BB–BC algorithm will optimize the (K_P, K_D, K_I) PID gains. The results of the parameter space approach are really PID gain ranges (K_P, K_D, K_I). As a result, the BB–BC optimization technique is applied in the construction of the optimal PID control, which

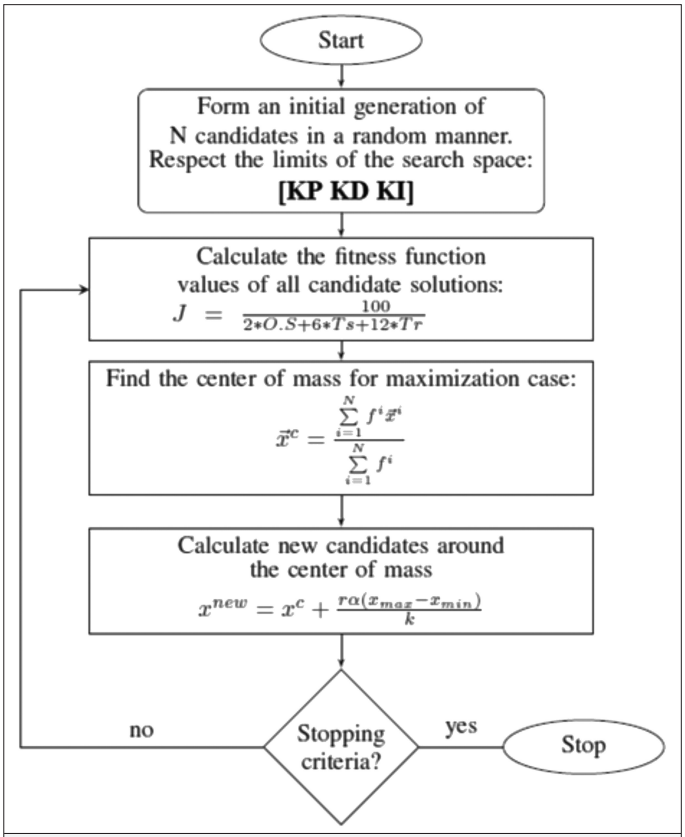

Fig. 11. Flowchart of the hypothesized method's Big Bang–Big Crunch optimization algorithm.

optimizes a time domain fitness function and thus avoids PID parameters that do not fulfill the extremize (minimize or maximize) the performance index function. The optimization approach is investigated in this report using a measurable performance index function that is inversely proportional to a dynamical system's time domain step response criterion to satisfy the shortest overshoot, fastest rise time, and quickest settling time. The following fitness function is suggested and utilized to guarantee all of these characteristics together [15]:

$$J = \frac{100}{2*O.S+6*T_s+12*T_r} \tag{48}$$

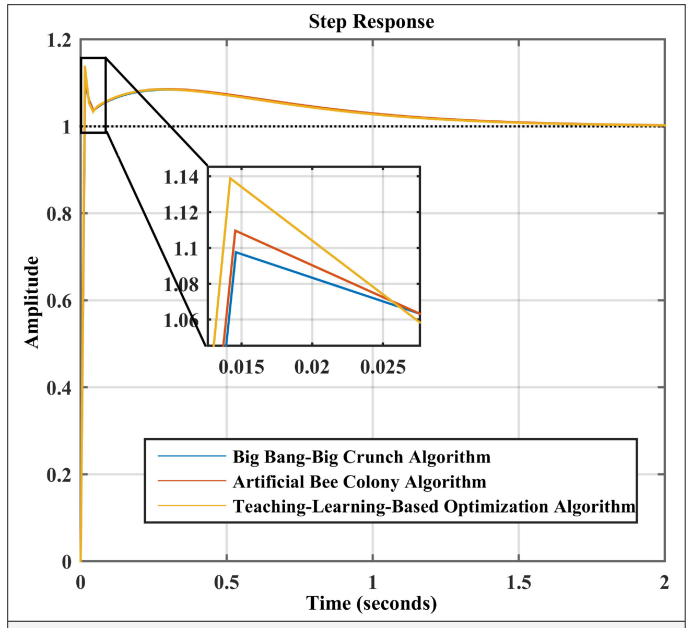

Fig. 12. Step response of Maglev for optimal values of proportional-integral-derivative (K_P, K_D, K_I) which is obtained by using the Big Bang–Big Crunch algorithm, artificial bee colony algorithm, and teaching-learning-based optimization algorithm when $R = q_1 = 50'$ and $L = q_2 = 0.2h$.

Because the fitness function is inversely proportional to a dynamical system's specific time domain step response requirements, the center of mass equation should be altered for the maximum case as follows:

$$\overleftarrow{x^c} = \frac{\sum_{i=1}^{N} \frac{1}{f^i} \overleftarrow{x^i}}{\sum_{i=1}^{N} \frac{1}{f^i}} \tag{49}$$

where the f^i is the fitness function J and the $\overleftarrow{x^i}$ is the matrix of PID gains controllers (K_P, K_D, K_I). The flowchart of BB–BC optimization algorithm is demonstrated in Fig. 11.

When the condition of the stopping criterion is fulfilled, the BB–BC algorithm will be stopped. The outcome of the BB–BC algorithm is the optimized matrix of PID gains controllers (K_P, K_D, K_I), which will

TABLE II. FOR THE GIVEN SYSTEM AND PICKING ALTERNATIVE VALUES OF UNCERTAIN PARAMETERS, THE PERFORMANCE VARIES IN OVERSHOT, RISING TIME, SETTLING TIME, AND PEAK TIME

Uncertain Parameter Values	Optimal Values of (KP,KD,KI)	Value of the Cost Function	*Tr* (seconds)	*Tp* (seconds)	OS (%)	*Ts* (seconds)
$q_1 = 45\ \Omega, q_2 = 0.15\ h$	(−11 372,−1617,−16 616)	4.48	0.01	0.28	7.7	1.1
$q_1 = 48\ \Omega, q_2 = 0.2\ h$	(−11 561,−1670,−16 470)	3.7	0.01	0.01	9.9	1.1
$q_1 = 50\ \Omega, q_2 = 0.18\ h$	(−11 458,−1654,−16 162)	4.07	0.01	0.29	8.6	1.1
$q_1 = 50\ \Omega, q_2 = 0.2\ h$	(−11 722,−1695,−16 590)	3.7	0.01	0.01	9.7	1.1
$q_1 = 52\ \Omega, q_2 = 0.22\ h$	(−11 634,−1699,−16 144)	3.02	0.01	0.01	12.8	1.2
$q_1 = 55\ \Omega, q_2 = 0.25\ h$	(−11 582,−1657,−16 178)	2.06	0.009	0.01	20.4	1.2

TABLE III. PERFORMANCE COMPARISON WHEN THE CERTAIN PARAMETERS $R=Q_1=50\ \Omega$ AND $L=Q_2=0.2$ H

Item	Big Bang–Big Crunch Algorithm	Artificial Bee Colony Algorithm	Teaching-Learning-Based Optimization Algorithm
Rise time (seconds)	0.01	0.0105	0.00997
Settling time (seconds)	1.1	1.17	1.14
Overshot (%)	9.7	11	13.9
Peak amplitude	1.097	1.11	1.14
Final value	1	1	1
Value of the cost function	3.7	3.4305	2.8746
Optimal values of (K_P,K_D,K_I)	(−11 722,−1695,−16 590)	(−11 566,−1665,−16 400)	(−11 683,−1643,−17 000)

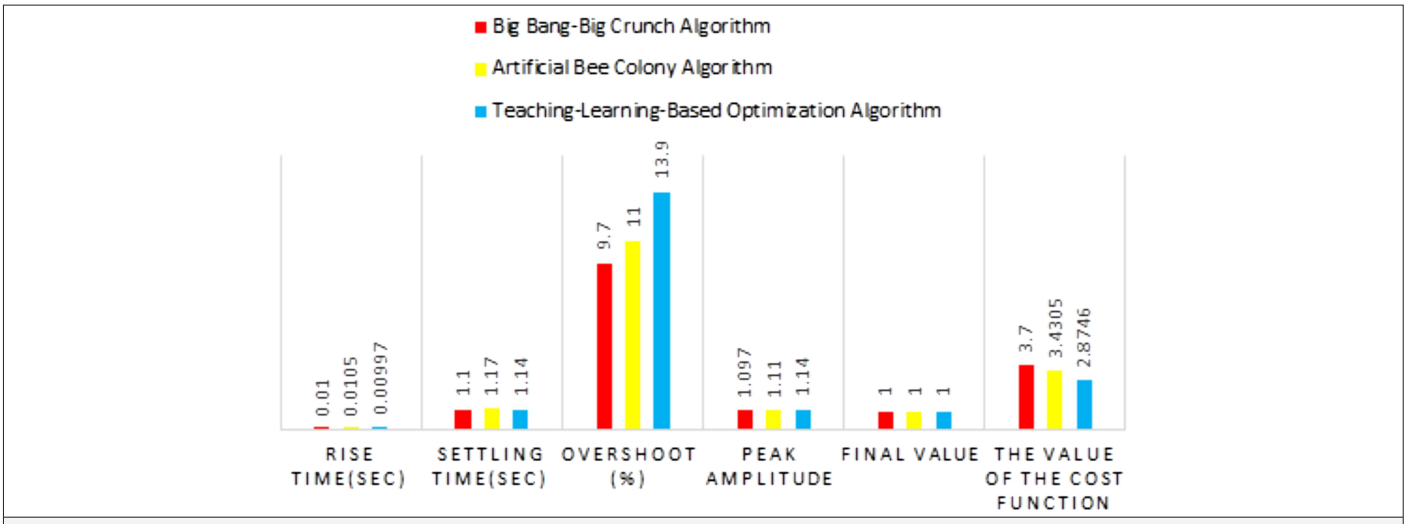

Fig. 13. Performance comparison with certain parameters $R=q_1=50\ \Omega$ and $L=q_2=0.2$ h using the Big Bang–Big Crunch algorithm, artificial bee colony algorithm, and teaching-learning-based optimization algorithm.

be used in the construction of PID controller that achieves the optimal cost function.

VI. RESULTS AND SIMULATION

The steps required to establish all stabilizing PID parameter regions for the ED-4810 Maglev system with certain and uncertain parameters were illustrated in section III. In this section, the BB–BC algorithm is used in order to elect an optimal of PID gains controllers (K_P,K_D,K_I) within stable region which maximizes the cost function. The search domains for (K_P,K_D,K_I) are selected to be (−12 000, −1700, −17 000) for lower bounds and (−11 000, −1600, −16 000) for upper bounds. The optimal matrix of PID gains controllers (KP,KD,KI) is derived after 25 iterations in the BB–BC algorithm. As seen in Table II, which highlights the disparities in overshot, rising time, settling time, and peak time for the given system and selecting different values of uncertain parameters within the given regions $45<q1=R<55$ and $0.15<q2=L<0.25$.

Moreover, Fig. 12 demonstrates step response at the optimal of PID gains controllers which are obtained by using the BB–BC algorithm, ABC algorithm, and TLBO algorithm with nominal values of uncertain parameters $R=q_1=50'$ and $L=q_2=0.2h$.

Table III and Fig. 13 compare the results of the (BB–BC) algorithm to some of the most well-known results of the ABC and TLBO algorithms. All of the methodologies listed in Table III and Fig. 13 have characteristics in common with (BB–BC) algorithm, including population-based features, nominal values of uncertain parameters $R=q_1=50'$ and $L=q_2=0.2h$, a significant number of iterations (more than or equal to 20 000) under a forgiving shutoff condition, and differential evolution constructions. We made an effort to compare all of these methodologies in a way that is reasonable, fair, and meaningful. The results show that the proposed controller using (BB–BC) algorithm outperformed other optimization algorithms.

VII. CONCLUSION

All stabilizing PID controller gains for the ED-4810 Maglev system benchmark (Maglev) are determined in this study in the presence of uncertain parameters by using a graphical parameter space technique. Within these stabilizing PID parameter domains, the BB–BC technique is utilized to identify the optimal parameter values for PID (K_P,K_D,K_I) controller. The BB–BC method aims to optimize a particular time domain performance index that is chosen to be inversely proportional to the dynamic system's step response characteristics (overshoot, settling time, rising time, and steady-state error). The

performance response of the ED-4810 Maglev is analyzed using MATLAB simulation to test the effectiveness of the suggested controller. This research showed that the proposed controller outperformed other optimization algorithms. Other algorithms could be utilized in the future to compare with the BB–BC algorithm outcomes.

Peer-review: Externally peer-reviewed.

Author Contributions: Concept – M.A.; Design – H.A.; Supervision – M.A.; Funding – K.I.; Materials – K.I.; Data Collection and/or Processing – K.I.; Analysis and/or Interpretation – M.A., H.A.; Literature Review – H.A.; Writing – K.I.; Critical Review – H.A.

Declaration of Interests: The authors have no conflicts of interest to declare.

Funding: The authors declared that this study has received no financial support.

REFERENCES

1. M. Almobaied, H. S. Al-Nahhal, and K. B. Issa, "Computation of stabilizing PID controllers for magnetic levitation system with parametric uncertainties," in International Conference on Electric Power Engineering-Pal estine (ICEPE-P). IEEE Publications; Gaza, Palestine: 2021, pp. 1–7.
2. M. Ahmed, M. F. Hossen, M. E. Hoque, O. Farrok, and M. Mynuddin, "Design and construction of a magnetic levitation system using programmable logic controller," *Am. J. Mech. Eng.*, vol. 4, no. 3, pp. 99–107, 2016.
3. S. K. Pandey, V. Laxmi *et al.*, "PID control of magnetic levitation system based on derivative filter," in Annual International Conference on Emerging Research Areas: Magnetics, Machines and Drives (AICERA/iCMMD). IEEE Publications; Kottayam, India: 2014, pp. 1–5.
4. D. Maji, M. Biswas, A. Bhattacharya, G. Sarkar, T. K. Mondal, and I. Dey, "Maglev system modeling and LQR controller design in real time simulation," in International Conference on Wireless Communications, Signal Processing and Networking (WiSPNET). IEEE Publications; Chennai, India: 2016, pp. 1562–1567.
5. B. Hamed, and H. Abu Elreesh, "Design of optimized fuzzy logic controller for magnetic levitation using genetic algorithms," *J. Inf. Commun. Technol.*, vol. 2, no. 1, 2012.
6. T.-E. Lee, J.-P. Su, and K.-W. Yu, "Implementation of the state feedback control scheme for a magnetic levitation system," in 2nd IEEE Conference on Industrial Electronics and Applications. IEEE Publications, 2007, pp. 548–553.
7. I. Ahmad, and M. A. Javaid, "Nonlinear model & controller design for magnetic levitation system," *Recent Adv. Signal Process. Robot. Autom.*, pp. 324–328, 2010.
8. N. F. Al-Muthairi, and M. Zribi, "Sliding mode control of a magnetic levitation system," *Math. Probl. Eng.*, vol. 2004, no. 2, pp. 93–107, 2004. [CrossRef]
9. J. Ackermann, *Robust Control: Systems with Uncertain Physical Parameters*. Springer Science & Business Media, 2012.
10. I. Ahmad, M. Shahzad, and P. Palensky, "Optimal PID control of magnetic levitation system using genetic algorithm," in IEEE International Energy Conference (ENERGYCON). IEEE Publications; Cavtat, Croatia: 2014, pp. 1429–1433.
11. M. Elsisi, and M. A. Ebrahim, "Optimal design of low computational burden model predictive control based on SSDA towards autonomous vehicle under vision dynamics," *Int. J. Intell. Syst.*, vol. 36, no. 11, pp. 6968–6987, 2021. [CrossRef]
12. M. Elsisi, M.-Q. Tran, H. M. Hasanien, R. A. Turky, F. Albalawi, and S. S. M. Ghoneim, "Robust model predictive control paradigm for automatic voltage regulators against uncertainty based on optimization algorithms," *Mathematics*, vol. 9, no. 22, p. 2885, 2021. [CrossRef]
13. M. Elsisi, and H. Abdelfattah, "New design of variable structure control based on lightning search algorithm for nuclear reactor power system considering load-following operation," *Nucl. Eng. Technol.*, vol. 52, no. 3, pp. 544–551, 2020. [CrossRef]
14. M. Elsisi, M. Soliman, M. A. S. Aboelela, and W. Mansour, "ABC based design of PID controller for two area load frequency control with nonlinearities," *Telkomnika Indonesian J. Electr. Eng.*, vol. 16, no. 1, pp. 58–64, 2015. [CrossRef]
15. M. Elsisi, "Optimal design of nonlinear model predictive controller based on new modified multitracker optimization algorithm," *Int. J. Intell. Syst.*, vol. 35, no. 11, pp. 1857–1878, 2020. [CrossRef]
16. D. T. Pham, A. Ghanbarzadeh, E. Ko, S. Otri, S. Rahim, and M. Zaidi, "The bees algorithm—A novel tool for complex optimisation problems," in *Intelligent Production Machines and Systems*. Amsterdam: Elsevier, 2006, pp. 454–459.
17. D. Teodorovic, and M. Dell'Orco, "Bee colony optimization–A cooperative learning approach to complex transportation problems," *Adv OR AI Meth Transport*, vol. 51, 2005, p. 60.
18. O. K. Erol, and I. Eksin, "A new optimization method: Big Bang–Big Crunch," *Adv. Eng. Softw.*, vol. 37, no. 2, pp. 106–111, 2006. [CrossRef]
19. M. J. Khan, D. Khan, S. J. Siddiqi, S. Saleem, and I. Khan, *Design & Control of Magnetic Levitation System ed-4810: Review and Stability Test*, 2019.
20. P. B. Dickinson, and A. T. Shenton, "A parameter space approach to constrained variance PID controller design," *Automatica*, vol. 45, no. 3, pp. 830–835, 2009. [CrossRef]
21. B. R. Barmish, and E. Jury, "New tools for robustness of linear systems," *IEEE Trans. Autom. Control*, vol. 39, no. 12, pp. 2525–2525, 1994.
22. T. Kumbasar, I. Eksin, M. Guzelkaya, and E. Yesil, "Adaptive fuzzy model based inverse controller design using BB-BC optimization algorithm," *Expert Syst. Appl.*, vol. 38, no. 10, pp. 12356–12364, 2011. [CrossRef]
23. S. Yılmaz, and M. G¨oka¸san, "Optimal trajectory planning by Big Bang-Big Crunch algorithm," in International Conference on Control., Decision and Information Technologies (CoDIT). IEEE Publications; Metz, France: 2014, pp. 557–561.
24. E. Dincel, and V. I. Genc, "A power system stabilizer design by Big Bang-Big Crunch algorithm," in 2012 IEEE International Conference on Control System, Computing and Engineering. IEEE Publications; Penang, Malaysia: pp. 307–312, 2012.
25. M. Almobaied, I. Eksin, and M. Guzelkaya, "Design of LQR controller with Big Bang-Big Crunch optimization algorithm based on time domain criteria," in 24th Mediterranean Conference on Control and Automation (MED). IEEE Publications; Athens, Greece: 2016, pp. 1192–1197.

Moayed Almobaied is an assistant professor of Electrical Engineering at the Islamic University of Gaza, Palestine. He received his B.Sc and M.Sc degrees in Control Engineering from the Islamic University of Gaza in 2001 and 2008, respectively. In 2017, he received Ph.D. in control and automation systems from Istanbul Technical University. He has received several fellowships including YTB and DAAD. His current research interests include robust control, optimal control, designing of modern control systems, nonlinear control systems, and robotics.

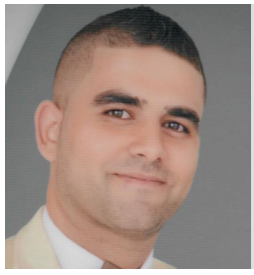

Hassan Sameer Al Nahhal was born on July 28, 1989, in Rafah, Palestine. He received a Bachelor degree in Electrical Engineering from the Islamic University of Gaza in 2012. Now, he is studying M.S degree in Control and Communications Systems from the same university. His current researches are on robust control systems, robotics control system, and nonlinear control systems.

Khaled Issa was born in Rafah, Libya. He received a Bachelor of Science degree in Electrical Engineering from the Islamic University of Gaza 7 years ago. Now, he is pursuing Master's in Electrical Engineering at the Islamic University of Gaza. Currently, he is working as Electrical Engineer for the Gaza Electricity Distribution Company for the past 6 years.